



OPEN

Investigating the expression changes of several key genes in prostate cancer cells under exposure to the ELF pulsed electromagnetic fields

Abouzar Bahari[✉], Javad Baharara, Khadijeh Nejad Shahrokhbadi & Maryam Lotfi

One of the less invasive methods in cancer treatment is the use of Extremely Low-Frequency Pulsed-Electromagnetic Fields (ELF P-EMF). In this study, after culturing and proliferating DU-145 prostate cancer cells, they were exposed to ELF P-EMF with different intensities and times. Then, the cells' viability was examined by applying the MTT test, and their level of apoptosis/necrosis was analyzed using a flow cytometry test. Then, for the studied groups, RNA extraction steps were performed, and cDNA was subsequently synthesized. Finally, using Real-time PCR, the expression levels of key genes such as PTEN, BAX, BCL-2, and MIR-21 in the targeted cancer cells were examined, and statistically, the significance of their expression differences with the control group was measured using SPSS software. The results indicated that by increasing the ELF P-EMF intensity from 22.6 to 35 mT and the duration of exposure, the mortality rate of cancer cells increased significantly. In addition, exposing cells of this line to ELF P-EMF could induce apoptosis in these cells. Also, applying fields with intensities of 22.6 and 35 mT led to a significant increase in the expression of the tumor suppressor gene PTEN and an increase in the expression of the apoptosis-inducing gene BAX. In addition, applying the field significantly reduced the expression of the oncogene MIR-21 and, to some extent, reduced the expression of the BCL-2 gene, which blocks apoptosis.

Keywords PTEN, BAX, BCL-2, MIR-21, Flow cytometry, MTT, RNA extraction, cDNA, Real-time PCR, SPSS

Currently, Prostate Cancer is the fourth leading cause of cancer death. This disease often presents with symptoms of urinary obstruction, etc. The disease usually grows very slowly. However, some types of this cancer grow rapidly and spread to other parts of the prostate gland or to the bones, lymph nodes, and lungs, which is very dangerous^{1,2}.

In cancer treatment, less invasive methods have always been considered. One of these methods is ELF-EMF (extremely low-frequency electromagnetic fields), which has been studied and researched for some cancers and has reduced the proliferation and destruction of cancer cells^{3,4}.

Grassi's 2004 study suggests that the potential effect of ELF on cancer cells involves the influence on the structure of cell membrane enzymes and the permeability of small molecules, rather than DNA damage⁵.

Also, according to Simkó's⁶ 2004 study and Simkó et al.⁷ cancer cells exposed to the waves release cytokines and reactive oxygen and nitrogen species, which lead to the instability of biological molecules. These substances affect intracellular signaling pathways and regulate the expression of specific genes involved in the inflammatory response, cell growth, differentiation, proliferation, and cellular stress response. Simkó also observed an increased induction of apoptosis in cancer cells after exposure to 50 Hz magnetic fields at 1 mT.

In research conducted by Sadooghi⁸ and Sadooghi et al.⁹ colon cancer cells of the HT-29 line, breast cancer cells of the MCF7 line, and normal L929 cells were exposed to low-frequency electromagnetic fields generated by alternating current of the urban network (with a frequency of 50 Hz and a voltage of 220 V) at different intensities. The results showed that the electromagnetic field with a frequency of 50 Hz and an intensity of 200

Department of Biology, Mashhad Branch, Islamic Azad University, Mashhad, Iran. [✉]email: aboozar.bahari@gmail.com

and 400 Gauss has inhibitory effects on growth and proliferation as well as cytotoxic effects on HT-29, MCF7 cancer cells, and normal L929 cells.

In a 2014 study by Filipovic et al. the effect of a 50 Hz EMF field on three cancer cell lines was investigated in vitro and by computer simulation: breast cancer MDA-MB-231, colon cancer SW-480, and HCT-116. After 24 h of incubation, the cells were exposed to a very low-frequency EMF of 50 Hz for 24 and 72 h. The experimental results clearly showed the disintegration of cells treated with the EMF of 50 Hz compared to untreated control cells. A large percentage of treated cells showed an increase in early apoptosis after 24 h and 72 h compared to the control group⁴.

The results of Pasi et al.'s study in 2016 showed that low-frequency magnetic fields can have a therapeutic effect on cancer patients and are effective in the epigenetic role of gene expression in cancer. They showed that magnetic fields with an intensity of 2 mT can play a role in autophagy in glioblastoma cells and affect the expression of microRNA genes that are effective in tumor progression in human cells. Their study also reported the effect of magnetic fields on the effectiveness of anticancer drugs and the epigenetic role of these fields on transcription factors of genes effective in tumor formation and mutations in genes involved in the DNA repair process¹⁰.

Ren et al. in 2017 showed that low-frequency magnetic fields are effective in lung cancer. In a mouse cancer model exposed to a 0.4 Tesla magnetic field for 35 days, they determined that the growth rate of cancer cells was reduced by inhibiting iron metabolism, which inhibited the cell proliferation cycle, and by stabilizing p53 protein and increasing miR-34 expression, it was able to affect the E2F1/E2F3 signaling pathway, and as a result, it inhibited lung cancer in mice¹¹.

Xu and his colleagues also conducted a similar study in a mouse lung cancer model in 2017. The results of their research showed that low-frequency magnetic field radiation can prevent tumor growth in mice and cause autophagy death of cancer cells, and this activation of autophagy was associated with increased expression of miR-486. This increased expression of miR-486 can inhibit the AKT/mTOR signaling pathway and inhibit lung cancer in mice. As a result of their research, the clinical application of these low-frequency magnetic fields against tumors and cancer treatment was reported¹².

A study by Koziorowska et al. in 2018 showed that ELF fields had different effects on U87-MG, B143 cancer cells as well as normal BJ and HEK cells exposed to different frequencies (2, 20, 30, 50, 60 Hz) and durations (0.5, 1, 2, 3 h), and cancer cells were much more damaged and destroyed³.

Calabró and magazù showed in 2019 that the destructive effects of ELF-EMF on cancer cells can be explained by the unfolding and aggregation of membrane proteins under exposure to electromagnetic fields, such that this radiation alters the function of cancer cells¹³.

In a study by Barati et al. in 2021, the effects of ELF-EMF on the levels of free radicals and calcium ions in breast cancer cell lines in BALB/c mice were investigated. For the first time, it was shown that necroptosis induction occurred in the MC4-L2 breast cancer cell line after exposure to ELF-EMF at a frequency of 1 Hz and an intensity of 100 mT for 2 h per day for 5 days¹⁴.

In a study by Shaygan et al. in 2022, the breast cancer cell lines BT-474 and the normal MCF10A were exposed to sinusoidal ELF-EMF at a frequency of 1 Hz and an intensity of 100 mT for 2 h per day for 5 days. The survival and apoptosis rates of these cells were measured by trypan blue and flow cytometry, respectively. Real-time PCR was also used to measure the mRNA expression levels of ER, PR, and HER2 genes. The data indicate that ELF-EMF induced about 69% apoptosis in BT 474 cells with a P-value of <0.05, but not in MCF10A. Also, the results of real-time PCR indicate a decrease in the expression of HER2 and PR and an increase in ER expression in the test group compared to the control group in BT-474 cells¹⁵.

Pantelis et al. (2024) investigated the antitumor properties of pulsed electromagnetic fields (P-EMFs) by irradiation on breast cancer epithelial cells (MCF-7 and MDA-MB-231) and normal fibroblasts (FF95). P-EMFs had a frequency of 8 Hz, a square wave type, and a magnetic flux density of 0.011 T and were applied twice a day for 5 days. The collected data showed that P-EMF reduced the proliferation and viability of breast cancer cells while having the opposite effect on normal fibroblasts. Furthermore, PEMF irradiation induced cell death and cellular senescence only in breast cancer cells, without having any effect on non-cancerous cells. These findings suggest P-EMF radiation as a novel, noninvasive anticancer strategy that, when combined with drugs, may destroy both cancer and remaining senescent cells, while simultaneously avoiding the side effects of current treatments¹⁶.

Considering the above, the necessity of this research and its importance in preventing the occurrence of the disease, which has a relatively high prevalence in different societies, as well as in treating sick individuals, is well understood. In fact, it is no secret that treating people with cancer using less invasive methods such as using extremely low-frequency electromagnetic fields (with very low energy according to the $E=hf$ relationship), has very few destructive effects on other tissues¹⁷, in terms of the spiritual impact it has on these individuals and their families, which it can improve human health, increase vitality in societies, and increase life expectancy.

In this study, we will first cultivate and proliferate DU-145 prostate cancer cells, and after reaching the appropriate density, passage, and seeding, we will expose them to a very low-frequency electromagnetic field with different intensities and times. Then, we will examine the cells' survival with the MTT test and the level of apoptosis or necrosis with the Flow cytometry test. Thereafter, for the control group and the groups exposed to the field, we will perform the steps of RNA extraction and purification, and then we will synthesize cDNA from it. Finally, using the Real-time PCR method, we will examine the expression level of key genes such as PTEN, BAX, BCL-2, and MIR-21 in DU-145 prostate cancer cells, and we will statistically measure the significant difference in their expression level with the control group at the 0.05 level using SPSS software.

We focused on the gene expression alterations of DU-145 prostate cancer cells under ELF P-EMF, specifically, the key genes related to cancer (suppressor genes, oncogenes, apoptosis-inducing genes, and microRNAs), to better understand how ELF P-EMF affects the expression of these key genes in the DU-145 cancer cell line. In

fact, we want to find out what the antitumor mechanisms of ELF P-EMF on this special cancer cell line are. These studies can also be very useful in investigating the best and optimized parameters of ELF P-EMF to treat prostate cancer, along with other kinds of therapies (like chemotherapy) or even without them (only by itself).

Materials and Methods

Preparation of an appropriate cell density of the DU-145 prostate cancer cell line

All experimental protocols were approved by the "Mashhad Medical Science Islamic Azad University" Research Ethics Committee on 6/11/2024, and all methods were carried out in accordance with relevant guidelines and regulations. Besides, all methods are reported in accordance with ARRIVE guidelines (<https://arriveguidelines.org>). Moreover, the source of DU-145 prostate cancer cells, used in this study is the Animal Development Applied Biology Research Center (Mashhad branch).

First, the appropriate culture medium was prepared by adding 10% FBS (from Gibco Company) + 1% antibiotic (Penicillin/ Streptomycin from Idea Zist Recombinant Company) to RPMI-1640 culture medium (from Idea Zist Recombinant Company). For example, to prepare 20 ml of culture medium, 2 ml of FBS and 200 μ l of antibiotic were added to RPMI-1640. Then, DU-145 prostate cancer cells (prepared in Animal Development Applied Biology Research Center (Mashhad branch)) were removed from the freezer (temperature -80 °C) and 1.5 ml of the culture medium prepared in the previous step was added to the cells. Next, the cells were centrifuged at 1500 rpm for 5 min to form a cell pellet. Then, the upper part of the cell pellet was discarded, and the cell pellet was mixed with an appropriate amount of culture medium until completely homogeneous. Afterwards, its contents were transferred to a 25 ml culture flask. An inverted microscope was used to examine and observe cell density, which was approved.

Passaging and seeding cells in 96-well plates

First, the cells were removed from the incubator, and then 300 μ l of Trypsin enzyme (from Idea Zist Recombinant Company) was added to the flask to detach the cells from the bottom of the dish. Of course, after the cells were separated from the bottom of the dish, twice the amount of enzyme was added to neutralize the effect of the enzyme. The separated cells were centrifuged at 1500 rpm for 5 min to precipitate and create a cell pellet. Then the upper part of the cell sediment was discarded. To prepare the cell plate, first, 10 μ l of the precipitated cells was removed and poured into the well, then 100 μ l of the culture medium was added to it, and 4 wells of the 96-well plate were filled in this way. Under an inverted microscope, the cell density of each plate was checked, which was confirmed.

Treatment of DU-145 cancer cells with ELF P-EMF

The electromagnetic field generation device consists of a 6000-turn copper coil, 30 cm long and 9.5 cm in diameter, which is powered by alternating urban electricity with a constant frequency of 50 Hz and a voltage of 220 V. Besides, it does not include a metallic core inside (its core is filled with air). In the path of the alternating city electricity, there is an electric converter, which regulates the intensity of the electric voltage and current entering the coil (Fig. 1).

In this study, the voltage intensity was set to 80 and 120 V AC, and given the coil resistance of about 86 ohms, the coil current intensity is 0.9 and 1.4 amps, respectively, but is generated alternatively based on the relationship $V=RI$. Therefore, the intensity of the electromagnetic field created, which is also intermittent (Pulsed EMF: P-EMF), is calculated based on the following relationship¹⁸:

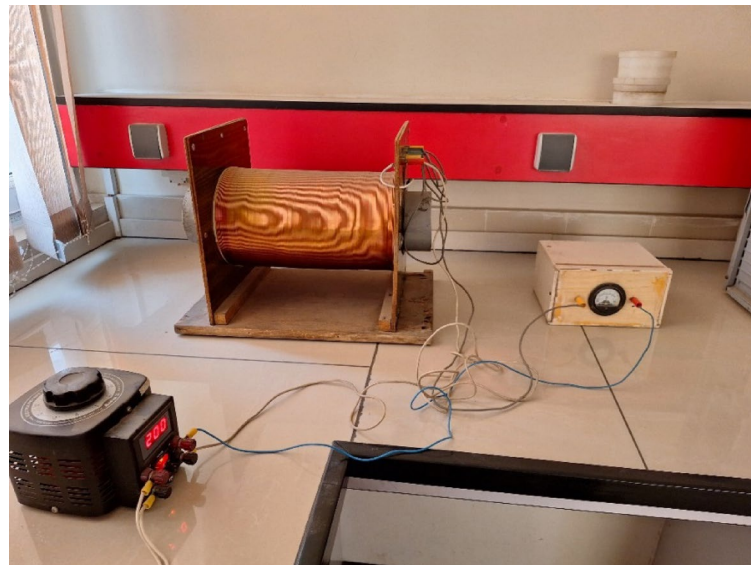


Fig. 1. Electromagnetic field generating device with city electricity frequency (50 Hz) and variable intensity.

$$B = \mu_0 n I = \mu_0 \frac{N}{L} I \quad (1)$$

where B : magnetic field strength in Tesla (T), N : number of turns of the coil, L : coil length in meters (m), I : current strength in amperes (A) and μ_0 : magnetic permeability constant of vacuum, whose value is equal to $4\pi \times 10^{-7}$.

For example, with a voltage of 80 V, which leads to a current strength of 0.9 A in the coil, according to the formula above, we have:

$$B = \mu_0 \frac{N}{L} I = 4\pi \times 10^{-7} \times \frac{6000}{0.3} \times 0.9 = 0.0226 \text{ T} = 22.6 \text{ mT}$$

Also, with a delicate Gauss meter, the calibration of the device was checked with different intensities to be in accordance with the above-mentioned formula, which was correct.

Therefore, the cells were divided into five groups: five 96-well plates, each filled with 4 wells of DU-145 cells, and each plate was placed inside and at the center of the coil to be exposed to the electromagnetic fields with a fixed frequency of 50 Hz and different intensities and times according to Table 1. It must be stated that we selected inside and at the center of the coil for cell positioning, since, according to the physics laws, this position possesses the maximum and most homogeneous electromagnetic field. Besides, the Voltage, Current, and Intensity of the EMF were measured and controlled during the exposure, using the Volt-meter, Ampere-meter, and Gauss-meter.

In addition, to analyze the homogeneity of the EM field applied to the cells, a software called FEMM (Finite Element Method Magnetics) version 4.2 was employed. This software is suitable for solving low-frequency electromagnetic problems on two-dimensional planar and axisymmetric domains by mathematical simulation using the Finite Element Method (FEM). FEMM addresses some limiting cases of Maxwell's equations¹⁹.

For our analysis, first, we defined a magnetic problem with the axisymmetric model and a frequency of 50 Hz. Then, we scheduled a cross-section of our coil in the software, using the coil dimensions and characteristics. Thereafter, the materials and blocks were defined in the software. The "18 AWG copper" for the coil wire (block 1) and the "air" for outside and inside of the coil (block 2). The circuit was also defined as a 6000-turn coil, and the boundaries were computed automatically by the software.

Then, the calculations were performed. Figure 2 represents the FEMM produced meshes and EMF strength (B) distribution of the employed coil for the voltage of 120 V, current of 1.4 A, and frequency of 50 Hz.

As can be understood in this figure, the EM field strength is almost homogeneous and constant (between 31 and 35 mT) inside the coil for the mentioned parameters. Hence, the homogeneity of the field for the mentioned cell groups was verified.

Investigating the viability of DU-145 cell lines using the MTT test

The MTT test is the most widely used method for assessing cell viability. The MTT assay can distinguish between live and dead cells by affecting intracellular organelles. This enzymatic method uses commonly available soluble tetrazolium salts as reaction substrates²⁰⁻²².

In our study, first, the tetrazolium salt (MTT) (from Sigma Company) was taken out of the freezer, and 10 μl of it was added to all samples exposed to the field and also to the control group. Then, these samples were placed in an incubator for 3 h, and after removing the supernatant, DMSO (from Gibco Company) was added. This solvent is added at the end of the experiment to dissolve the formazan crystals, and this allows the absorption spectrum of the solution to be measured. After that, the viability of the cells was examined by a spectrophotometer. Since the mortality rate of cancer cells increased with increasing the duration of exposure to the field (60 min), this effect may have been due to the increase in temperature to above 43 °C (it was measured by a thermometer), which caused cell denaturation. Therefore, for the next steps, only cells that were exposed to a constant frequency and variable intensity electromagnetic field for 30 min, i.e., groups 2 and 3 in Table 1, were selected, and groups 4 and 5 of this table were eliminated.

Examining the percentage of apoptotic/necrotized cells using flow cytometry (Annexin V/ PI)

First, the cells of the control group, 2 and 3 of Table 1, were separated from the dish using the enzyme Trypsin and then neutralized by adding twice the culture medium. Then, the cells of each group were centrifuged at a speed of 3000–4000 rpm for 5 min. After the liquid above it was discarded, the cell pellet was dissolved in 500 μl of Binding buffer. Afterwards, 2 μl of Annexin V and 1 μl of PI (Propidium iodide) (both from Mahboub

Group	Voltage, V	Current, A	Maximum Electromagnetic intensity (B) inside the coil, mT	Time of electromagnetic exposure, min
1 (Control)	–	–	–	–
2	80	0.9	22.6	30
3	120	1.4	35	30
4	80	0.9	22.6	60
5	120	1.4	35	60

Table 1. Exposure of 5 DU-145 cell groups to an electromagnetic field with a fixed frequency of 50 Hz and different intensities and times.

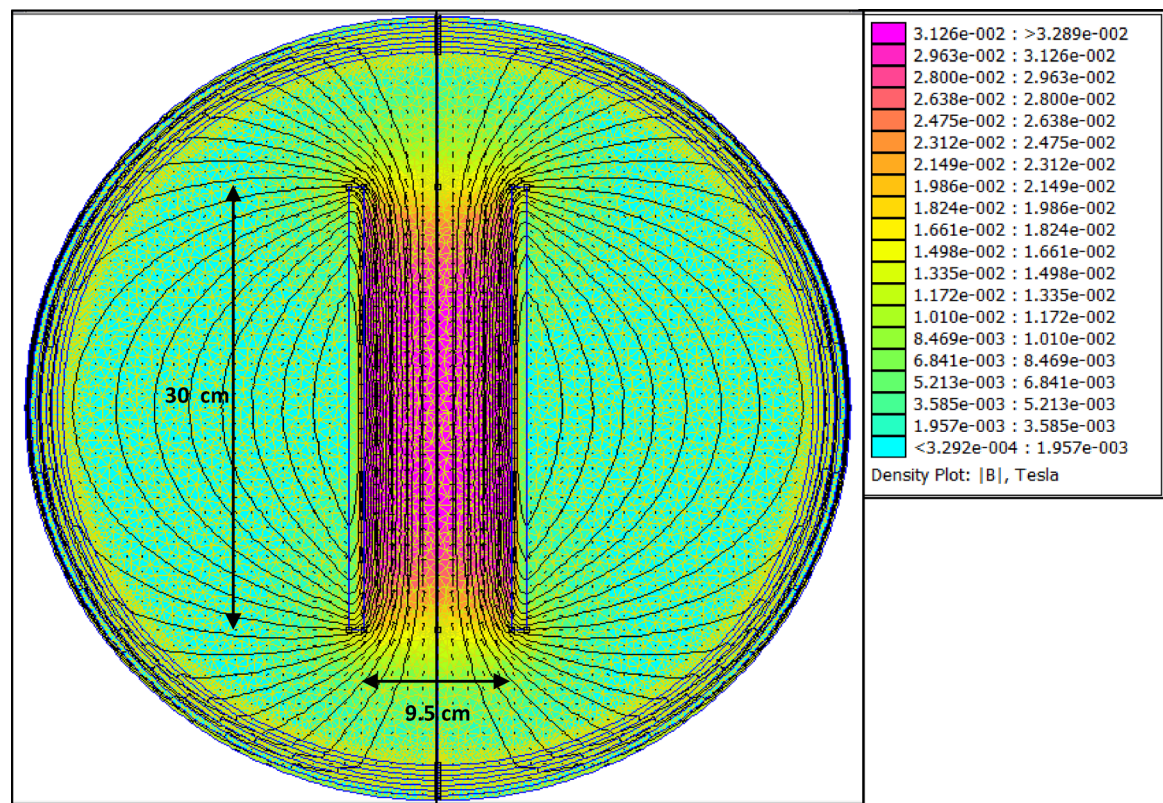


Fig. 2. The FEMM produced meshes and EMF strength (B) distribution of the employed coil for the voltage of 120 V, current of 1.4 A, and frequency of 50 Hz.

Bioresearch Company) were added for 10 min. Then, the amount of necrotic and apoptotic cells in each group was examined in a flow cytometer.

RNA extraction and purification steps

To extract RNA, the process usually begins with lysing the cells using a buffer, such as RNA lysis buffer (RL solution), which is specifically designed for RNA purification. This is highly denaturing and typically consists of phenol and guanidine isothiocyanate. RNase inhibitors are usually present in the lysis buffer because RNases can be very resistant to denaturation and remain active²³.

Based on the RNA extraction kit of the Pars Tous Company²⁴, first, the cells of the control group, 2 and 3 of Table 1, were separated from the dish using the enzyme Trypsin and then neutralized by adding twice the culture medium. These cells were transferred to small Eppendorf tubes. Then, the cells of each group were centrifuged at 3000–4000 rpm for 5 min. After the liquid on it was discarded, the cell pellet was mixed in 750 μ l of RL solution. Then, 150 μ l of chloroform was added to improve phase separation and shaken for 15 s. This mixture was centrifuged in a refrigerated centrifuge at 4 °C at 13,000 rpm for 12 min. The result will be three phases, with RNA, which is the lightest, at the top, DNA in the middle, and proteins, which are heavier, at the bottom. The upper phase (RNA), about 200 μ l, was extracted, and the same amount (200 μ l) of 70% ethanol (from Hayan Teb Company) was added to it to precipitate the nucleic acids from the solution²⁵.

For RNA purification, the mixture was transferred to a spin column equipped with a filter and centrifuged again in a refrigerated centrifuge at 13,000 rpm for 1 min. The fraction formed under the filter containing RNA was then extracted. For RNA re-purification, 700 μ l of isopropanol (PW) was added to the fraction containing RNA from the previous step and centrifuged again in a refrigerated centrifuge at 13,000 rpm for 1 min. The fraction formed under the filter containing RNA was then extracted. The previous step was repeated once more with 500 μ l of isopropanol (PW), and the fraction formed under the filter containing RNA was extracted. This time, only the Eppendorf-containing RNA was centrifuged in a refrigerated centrifuge at 13,000 rpm for two minutes, and the fraction formed under the filter containing pure RNA was extracted. The resulting RNA was transferred to a new Eppendorf tube, and 50 μ l of DEPC-treated water was added. Then it was placed for 3 min at room temperature, and then again for 1 min in a refrigerated centrifuge at 13,000 rpm.

The amount of RNA in each group was quantified by the Nanodrop (a kind of spectrophotometer device). Then, the Eppendorf was placed in the freezer (temperature –80 °C) to continue working.

Synthesis of cDNA from extracted RNA

cDNA (complementary DNA) is a synthetic DNA that is transcribed from a specific mRNA through a reaction using the enzyme reverse transcriptase. While DNA is made up of both coding and non-coding sequences,

Group	RNA mass, μ g	RNA volume, μ l	Buffer Mix, μ l	Enzyme Mix, μ l	DEPC-treated water, μ l	Total volume, μ l
1 (control)	0.097	1	10	2	7	20
2 (under EMF of 22.6 mT in 30 min)	0.041	2.36	10	2	5.64	20
3 (under EMF of 35 mT in 30 min)	0.048	2.02	10	2	5.98	20

Table 2. Amounts of Buffer Mix, Enzyme Mix, and DEPC-treated water, added to the extracted RNA for cDNA synthesis according to Pars Tous Company's instructions.

Gene name	Forward primer	Reverse primer
GAPDH (internal control gene)	TGACTTCAACAGCGACACC	TTGCTGTAGCCAAATTCTGTT
BAX	TTTGCTTCAGGGTTCATCCA	CTCCATGTTACTGTCCAGTCGT
BCL-2	TGTGTGGAGAGGGTCAACCG	GGATAACGGAGGCTGGATGC
PTEN	TGGAGGCTATCAACAAAGAATGGG	CATTGCTGAAGAGGTAGAGGACAC
SNORD (internal control gene)	ATCACTGTAAAACCGTT	
MIR-21	GGCTTGTCAAGACTGTATGT	

Table 3. Sequence of primers used, manufactured by SinaClon Company.

cDNA contains only the coding sequences. Using the enzyme reverse transcriptase, a single-stranded copy of the cDNA is produced. This can then be made into double-stranded cDNA by a DNA polymerase and fed into a standard PCR-based amplification process.

RNA must be converted to cDNA for real-time quantitative PCR (RT-qPCR) testing because cDNA is more stable and can be efficiently replicated as a template during the PCR process^{26,27}.

According to these explanations, the steps for this section were as follows:

First, the container containing each group's RNA was removed from the freezer, and then, for each group, according to the Pars Tous Company cDNA synthesis kit²⁸, some amounts of Buffer Mix, Enzyme Mix, and DEPC-treated water were added to them according to Table 2.

Buffer mix for cDNA synthesis contains a reverse transcriptase enzyme, dNTPs (deoxynucleotide triphosphates), and the required primers along with a stabilizer. These molecules act as a substrate for the reverse transcriptase enzyme during cDNA synthesis. Three primers that are used in the Buffer mix include Oligo(dt), Random hexamer, and Specific.

The Enzyme mix also contains a reverse transcriptase enzyme called Moloney murine leukemia virus (MMLV) reverse transcriptase (RT) that is thermally stabilized with an RNase inhibitor and stabilizer.

It should be noted that it is very important to follow the manufacturer's instructions for specific buffer combinations and reaction conditions. According to the program mentioned in the kit, the above-prepared mixture was placed in the Thermal-cycler for each group:

- Incubate 10 min @ 25 °C
- Incubate 60 min @ 47 °C
- Stop reaction by heating for 5 min @ 85 °C

Then, the cDNAs of each group were removed from the device and placed in the freezer.

Performing a real-time PCR test

Today, RT-qPCR is commonly used to measure and compare RNA levels due to its accuracy, reproducibility, specificity, sensitivity, and high throughput²⁹. In this technique, in order to quantify the data obtained from measuring mRNA levels, the amount of target mRNA can be measured relative to the amount of mRNA of an internal control gene³⁰. Housekeeping genes are usually described as “essential components for cellular existence regardless of their specific function in the tissue or organism” and are stably expressed regardless of tissue type, developmental stage, cell cycle status, or external signal³¹.

A gene that is sometimes applied as a housekeeping gene is the GAPDH, which encodes the enzyme Glyceraldehyde 3-phosphate dehydrogenase in humans. This enzyme plays a role in breaking down sugar molecules and providing energy. This enzyme also plays a role in several other non-metabolic processes. Some sources have suggested that GAPDH may not be a good choice for a housekeeping gene, but we used it as an internal control gene in real-time PCR anyway³². In addition, SNORDs, especially SNORD48, have been frequently used as reference genes in studies investigating miRNA expression in prostate cancer tissues. They are small nuclear RNAs (snoRNAs) that are known for their stability and constant expression levels. This makes them suitable for normalizing gene expression data in cancer research^{33–35}.

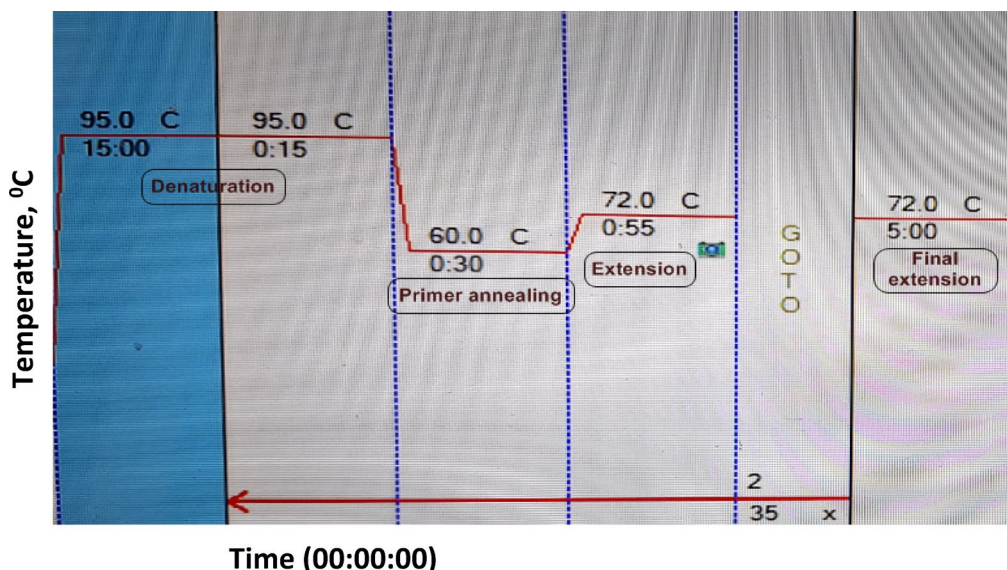
Hence, to perform this experiment, first, the necessary primers for the internal control gene and the genes whose expression levels should be examined were purchased. The sequences of the primers used, manufactured by SinaClon Company³⁶, are shown in Table 3.

Then, the primers were diluted for each gene in separate microtubes as shown in Table 4.

Gene name	micro-tube No	Water volume, μ l	Forward primer volume, μ l	Reverse primer volume, μ l
GAPDH (internal control gene)	1	36	2	2
BAX	2	36	2	2
BCL-2	3	36	2	2
PTEN	4	36	2	2

Table 4. Dilution of primers for the studied genes and their internal control genes.

Gene name	Water volume, μ l	Forward primer volume, μ l	Reverse primer volume, μ l	Syber Green mixture volume, μ l	cDNA volume, μ l	Total volume, μ l
GAPDH (internal control gene)	7	1	1	10	1	20
BAX	7	1	1	10	1	20
BCL-2	7	1	1	10	1	20
PTEN	7	1	1	10	1	20
SNORD (internal control gene)	8	0.5	0.5	10	1	20
MIR-21	8	0.5	0.5	10	1	20

Table 5. Master Mixes prepared for the studied genes and internal control genes according to the instructions of Pars Tous Company.**Fig. 3.** The temperature and time schedule announced by the primer manufacturer (SinaClon Company) that gene expression in the BioRad Real-time PCR device was performed according to this schedule.

However, the primers for the SNORD (internal control gene) and MIR-21 genes were already pre-prepared and did not require dilution, and were directly added to the Master Mix.

To make the Master Mix, the instructions of the cDNA synthesis kit manufacturer had to be followed. Therefore, according to the instructions of Pars Tous Company, the Master mixes for each gene were prepared according to Table 5 in the proportions mentioned. It must be mentioned that Syber Green mixture, including Syber Green and Taq polymerase was provided from Pars Tous Company.

Since we have three groups (1 (control), group 2, and group 3) and for each, three repetitions are performed, a total of 9 micro-tubes were prepared with the total volume and ratios mentioned in the table above. The prepared Master Mixes were positioned in the BioRad Real-time PCR device and were placed according to the temperature and time program announced by the primer manufacturer (SinaClon Company) as depicted in Fig. 3.

Results and discussions

Images of DU-145 cancer cells treated with ELF-EMF

After exposing the DU-145 cancer cells to two different intensities of electromagnetic fields and a fixed frequency of 50 Hz, the cell density was examined with an inverted microscope. Figs. 4, 5, 6 indicate the images of DU-145 cancer cells of the control group (not exposed to the field), exposed to a field of 50 Hz frequency and 22.6 mT intensity for 1 hour, and exposed to a field of 50 Hz frequency and 35 mT intensity for 1 hour, respectively, at 40X magnification of the inverted microscope. As can be seen in these images, a large portion of the cells exposed to intensities of 22.6 and 35 mT for 1 hour were killed. The cause of this problem is the effect of the electromagnetic field, plus the high heat generated (about 60 °C) by the electric current passing through the copper wires of the coil.

Results of MTT assay and statistical analysis

The results of the MTT test (percentage of viability) of DU-145 cancer cells under a very low-frequency field of 50 Hz and two intensities of 22.6 and 35 mT for 30 and 60 minutes (groups 2, 3, 4, and 5) and comparison with the control group (group 1) were obtained and these data were given as input to SPSS version 26 software. Then, using the One-way ANOVA test, the significance of the difference in cell viability between the field and the control group was examined based on a *P*-value below 0.05 with one star (*), below 0.01 with two stars (**), and below 0.001 with three stars (***)�

According to these results, since the Significance (*P*-value) is zero in comparison between the other groups and the control group (it receives a three-star (***)) mark), this indicates a very significant difference between the percentage of cell viability under the ELF P-EMF at the mentioned intensities and the control group. Fig. 7 shows the Column chart for the MTT results of DU-145 cells under the field with a frequency of 50 Hz and two different intensities and times, along with error bars and the significance of the difference in cell viability compared to the control group based on the *P*-value.

As shown in this chart, with increasing field intensity, the mortality rate of cancer cells increased significantly. Also, with increasing the exposure time to 60 min under the field, the mortality rate of cancer cells increased significantly again, but this effect was probably due to the increase in temperature to about 60 °C (it was measured by a thermometer), which caused damage to the cells. Therefore, for the next steps, only cells that were exposed to the electromagnetic field for 30 min were selected to eliminate the effect of temperature.

It is also possible to statistically compare the results between groups 2, 3, 4, and 5 pairwise. According to the One-way Anova test, only group 5 (35 mT field intensity group for 60 min) had a significant difference in cell mortality compared to the other groups, which, as mentioned, is probably partly due to the high temperature recorded (more than 60 °C).

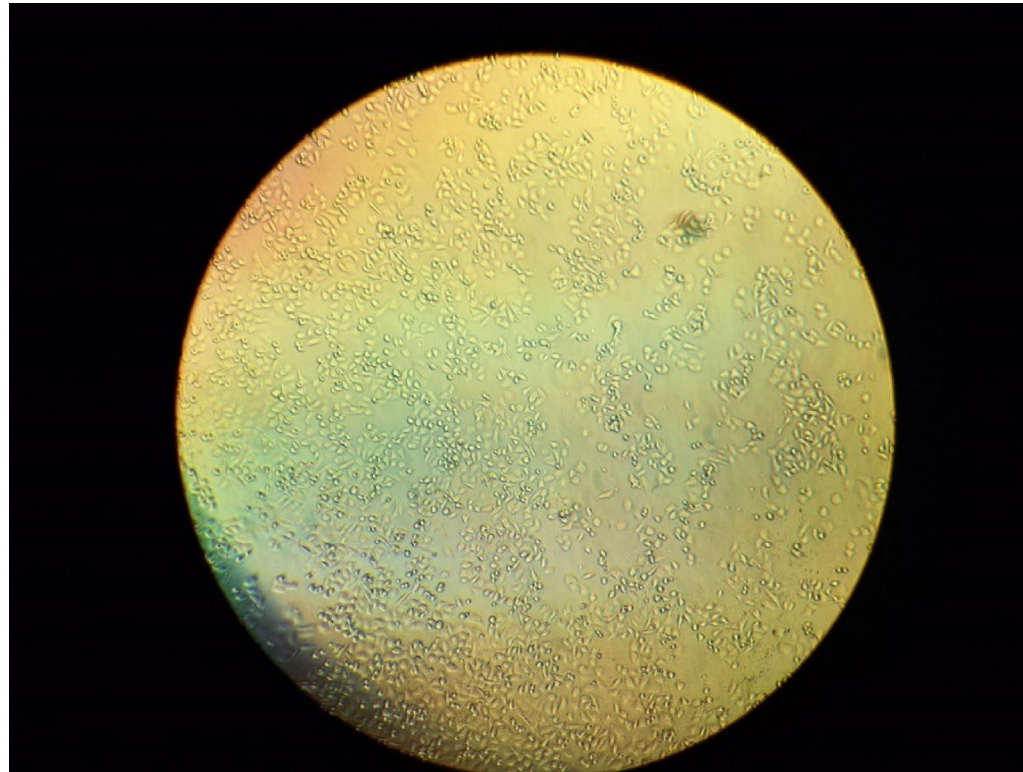


Fig. 4. Image of DU-145 cancer cells in the control group (not exposed to the field) with an inverted microscope at 40X magnification.

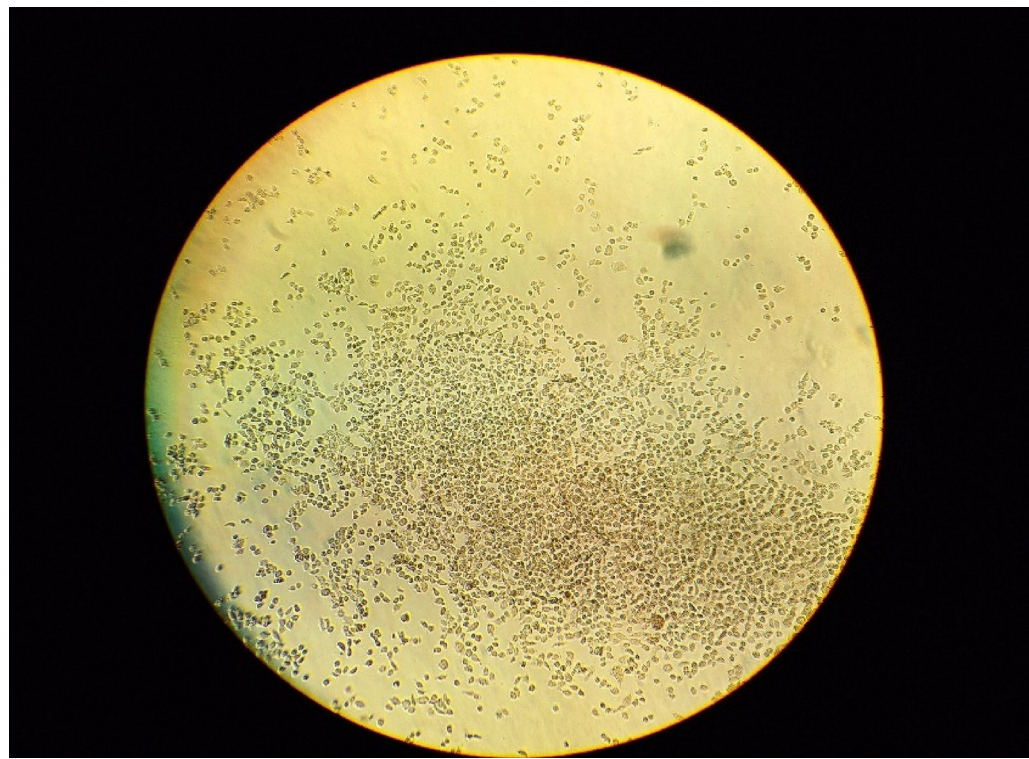


Fig. 5. Image of cancer cells exposed to a field with a frequency of 50 Hz and an intensity of 22.6 mT for 1 h at 40X magnification of the inverted microscope.

Results of the flow cytometry test

Figures 8, 9, 10 represent the results of the flow cytometry test, performed on DU-145 cancer cells for the control group, the groups under the ELF P-EMF with a constant frequency of 50 Hz and the intensity of 22.6 mT and 35 mT for a period of 30 min, respectively. It should be noted that in these flow cytometry graphs, FL1-H refers to Annexin V and FL2-H refers to propidium iodide (PI).

As can be seen in Figs. 7, 8, 9, for the control group that was not exposed to the field, most of the cells were healthy (84%) and were located in the Q4 region, and only 16% were located in other regions. However, for the group that was exposed to a field of 22.6 mT for 30 min, about 36.5% were located in the Q2 and Q3 regions, i.e., the primary and secondary apoptosis regions, and the percentage of cells that underwent pure necrosis (Q1 region) was very low (0.26%). Also, for the group that was exposed to a field of 35 mT for 30 min, about 65% were located in the Q2 and Q3 regions, i.e., the primary and secondary apoptosis regions, and the percentage of cells that underwent pure necrosis (Q1 region) was very low (0.85%).

This experiment proves that exposure of DU-145 prostate cancer cells to a very low-frequency EMF of 50 Hz with two intensities of 22.6 and 35 mT can induce apoptosis in these cells.

Of course, in terms of the effect of temperature caused by the electromagnetic field, it should be noted that necrosis occurs at a temperature of 50 °C or higher, while apoptosis occurs in the range of 43–50 °C^{37–39}. Therefore, given that exposure of this cell line to the field with the aforementioned intensities for 30 min does not lead to a temperature higher than 43 °C (it was measured by a thermometer), neither apoptosis nor necrosis occurs due to the high temperature caused by the field.

RNA extraction results and purification

Figure 11 shows a three-phase image of the RNA extraction solution after lysing the cells using a lysis buffer, adding chloroform to the solution, and placing the solution in a refrigerated centrifuge. In this image, RNA, which is the lightest, is clearly and beautifully differentiated from the DNA (in the middle) and proteins, which are heavier (at the bottom).

After performing RNA extraction steps (according to the manufacturer's kit) using the materials, tools, and devices mentioned in the previous chapter, the quantitative RNA mass/ volume values for each group were obtained according to Table 6.

Results of the real-time PCR test and statistical analysis

Figure 12 represents the column chart of relative normalized expression values of BAX, BCL-2, and PTEN genes (relative to internal control gene GAPDH) as well as the results of MIR-21 gene expression values (relative to internal control gene SNORD) along with the error bars (their standard deviation (SD) values) for the control group and the groups under the field with intensities of 22.6 and 35 mT.

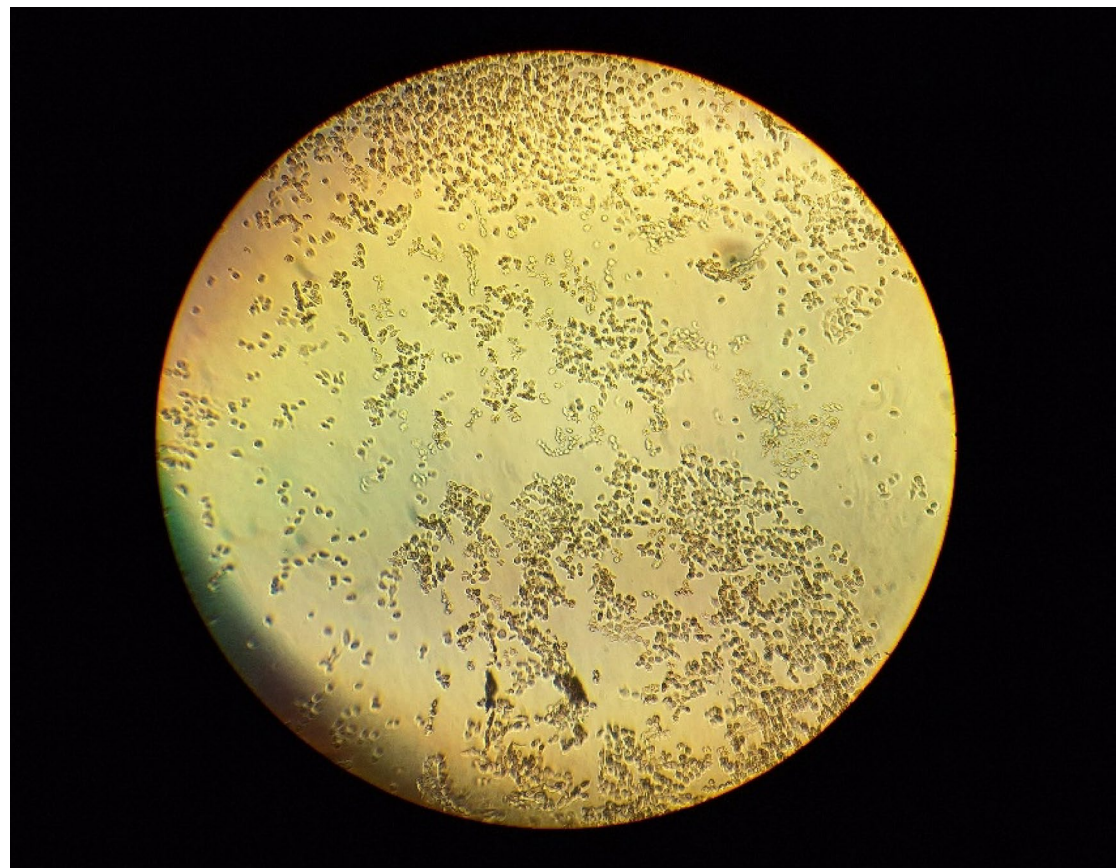


Fig. 6. Image of cancer cells exposed to a field with a frequency of 50 Hz and an intensity of 35 mT for 1 h at 40X magnification of the inverted microscope.

For the statistical analysis of the Real-time PCR, the data obtained from the test, along with the standard deviation (SD) values, were entered as input into SPSS version 26 software.

Then, using the One-way ANOVA test, the significance of the difference in genes' relative expression between the groups under ELF P-EMF and the control group was examined based on *P*-values: below 0.05 with one star (*), below 0.01 with two stars (**), and below 0.001 with three stars (***) were marked.

Figure 13 reveals a screenshot of the results of the One-way ANOVA test in SPSS software on the significance of the difference in gene's relative expression between the groups under ELF-EMF and the control group.

The results of this test show that for the PTEN gene, the *P*-value for both field intensities of 22.6 and 35 mT is below 0.05 (*) and therefore there is a significant difference between the relative expression values of this gene under the field with these intensities and the control group. Also, for the MIR-21 gene under the electromagnetic field with an intensity of 35 mT, there is a significant difference in this regard (*P*-value less than 0.05).

It should be noted that the PTEN enzyme is a phosphatase in humans and is encoded by the PTEN gene. The mutation of this gene leads to the development of many cancers, including prostate cancer, because PTEN acts as a tumor suppressor gene through the function of its protein phosphatase product, and this phosphatase plays a role in regulating the cell cycle and prevents rapid cell growth and division⁴⁰. In addition, PTEN mutations in the genetic class cause hereditary syndromes that lead to an increased risk of tumors⁴¹.

Hence, applying fields with intensities of 22.6 and 35 mT at a constant frequency of 50 Hz for 30 min resulted in a significant increase in the expression of the tumor suppressor gene PTEN (*), and as a result, it can be said that applying fields with the above intensities and frequencies is effective in suppressing prostate cancer tumors, and with increasing field intensity, the expression of this gene also increases. Figure 14 reveals the Real-time PCR output results showing the relative expression of the PTEN gene for the two groups under field intensities of 22.6 and 35 mT and the control group, as well as their standard deviation (SD) and one, two, or three stars for *P*-values.

Besides, it is necessary to explain that apoptosis, as a major physiological mechanism of cell death, plays an important role in maintaining homeostasis in tissues. Reduced apoptosis disrupts the balance between cell proliferation and cell death, leading to increased susceptibility to tumors^{42,43}. The BAX gene is responsible for producing a protein that regulates apoptosis by inducing it (pro-apoptotic) and is a member of the BCL-2 gene family. This gene is involved in p53-mediated apoptosis⁴⁴. Increased apoptosis and BAX expression, not BCL-2 or the BAX/BCL-2 ratio, may play a role in the relatively lower incidence of human small intestinal carcinoma⁴⁵.

Figure 15 reveals the Real-time PCR output results showing the relative expression of the BAX gene for the two groups under field intensities of 22.6 and 35 mT and the control group, as well as their standard deviation

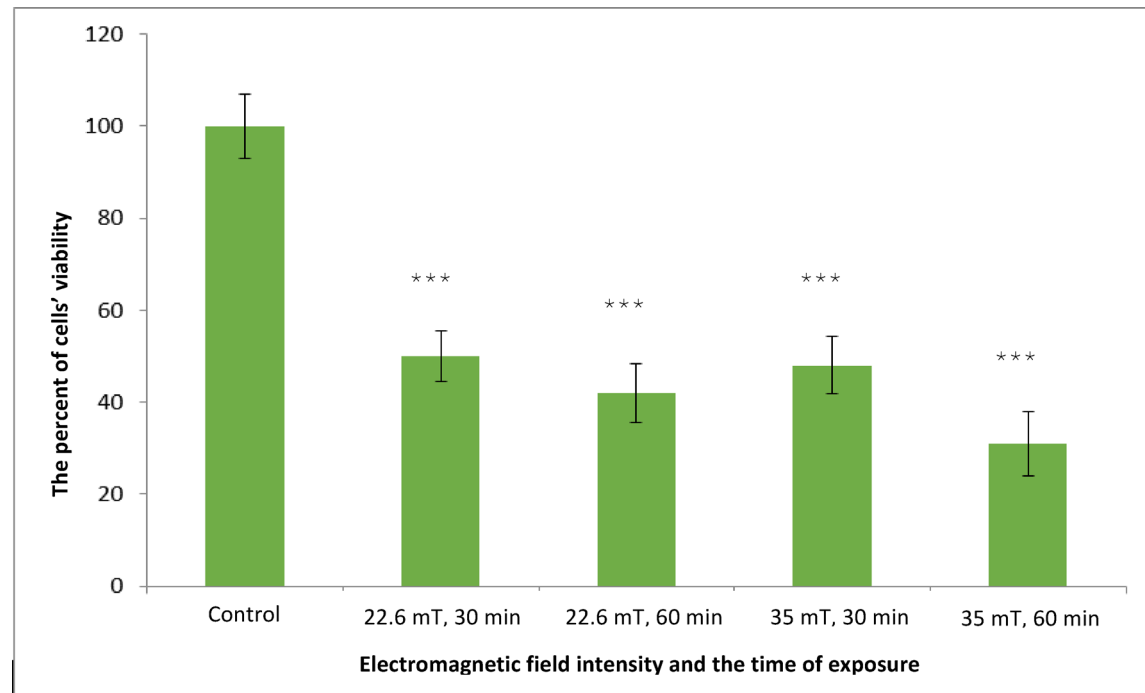


Fig. 7. The Column chart for the MTT results of DU-145 cells under a field with a frequency of 50 Hz and two different intensities and times along with error bars and significance of the difference in cell viability compared to the control group based on *P*-value (below 0.05 with one star (*), below 0.01 with two stars (**) and below 0.001 with three stars (***)).

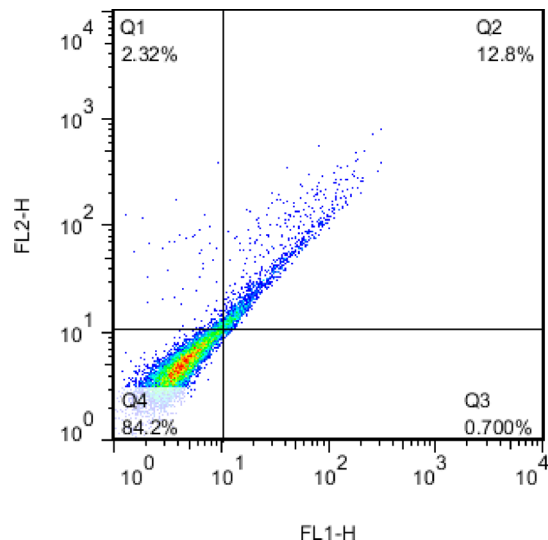


Fig. 8. Flow cytometry test results, performed on DU-145 cells for the control group: Most of the cells are healthy (84%) and are located in the Q4 segment.

(SD). As can be revealed in this figure, being a magnified version of Fig. 11 for the BAX gene, applying fields with the mentioned conditions increases the expression of the pro-apoptotic gene BAX, although this increase is not significant compared to the control group. As a result, it can be said that applying fields with the above intensities and frequencies is somewhat effective (if we consider the average amount of relative gene expression) in inducing apoptosis of prostate cancer cells by this gene and reducing tumor growth, and with increasing field intensity, the relative expression of this gene increases somewhat.

Importantly, the ability of P53 to promote cell death can be directly related to its tumor suppressor function. Only in the last decade have the targets of the p53 protein in apoptosis been considered. It now appears that the primary action of p53 in apoptosis is to, directly and indirectly, regulate the activity of Bcl-2 family proteins.

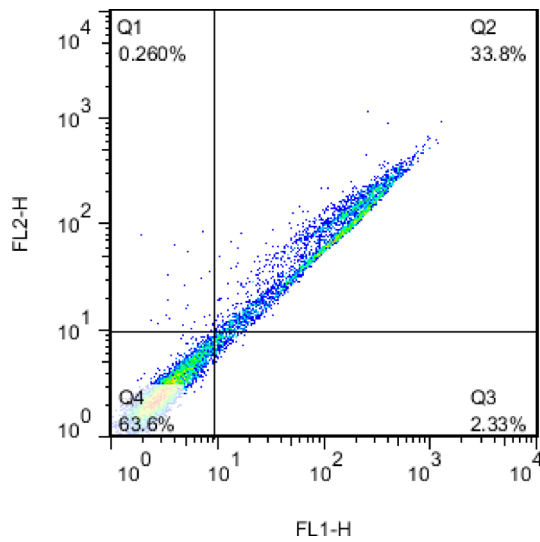


Fig. 9. Flow cytometry test results performed on DU-145 cells for the group under ELF P-EMF with a constant frequency of 50 Hz and intensity of 22.6 mT for 30 min: About 36.5% are located in the Q2 and Q3 regions, i.e. the primary and secondary apoptosis regions and the percentage of cells that have undergone pure necrosis (Q1 region) is very low.

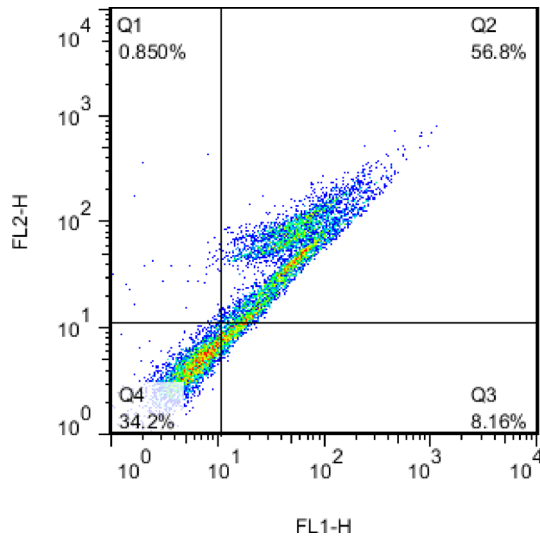


Fig. 10. Flow cytometry test results performed on DU-145 cells for the group under ELF P-EMF with a constant frequency of 50 Hz and intensity of 35 mT for 30 min: About 65% are located in the Q2 and Q3 areas, i.e. the areas of primary and secondary apoptosis, and the percentage of cells that have undergone pure necrosis (area Q1) is very low.

p53 directly induces BAX transcription. Furthermore, induction of BAX by stress-activated p53 can overcome the anti-apoptotic effects of Bcl-2⁴⁶. In general, the normal P53 gene, which produces the p53 protein, can limit cell proliferation after DNA damage by two mechanisms: cell cycle arrest (tumor suppressor) or activation of apoptosis, with mutations in this gene disrupting these mechanisms⁴⁷. The importance of p53 for chemosensitivity is confirmed by the fact that currently, the most treatable cancers are among the minority of tumors in which p53 is not mutated, namely some tumors of hematopoietic and germ cells^{48,49}.

Given that BAX gene expression is regulated by the tumor suppressor p53 and that this gene is involved in p53-mediated apoptosis, it can be said that applying fields with intensities of 22.6 and 35 mT at a constant frequency of 50 Hz for 30 min is likely (if we consider the average amount of relative gene expression) to lead to increased expression of the tumor suppressor gene P53 and, as a result, is also somewhat effective in suppressing prostate cancer tumors by the P53 gene.

It is necessary to explain that microRNAs are small, non-coding RNA molecules that affect many important cellular processes, including early development, cell differentiation, proliferation, and apoptosis, by regulating

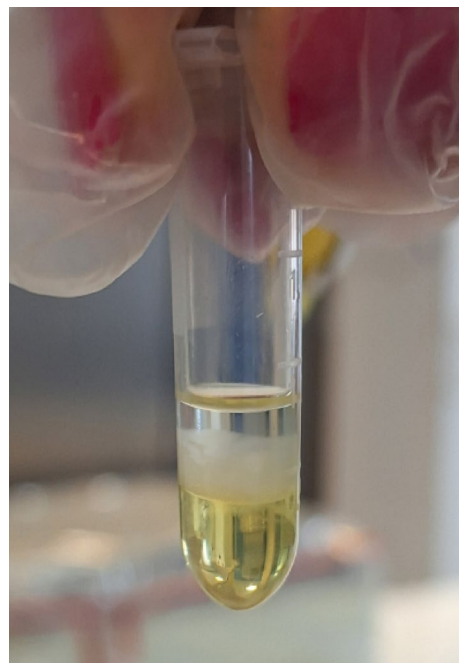


Fig. 11. An image of the three-phase formation of the RNA extraction solution after going through its extraction steps.

Group	RNA mass, μg	RNA volume, μl
1 (control)	0.097	1
2 (under EMF = 22.6 mT in 30 min)	0.041	2.36
3 (under EMF = 35 mT in 30 min)	0.048	2.02

Table 6. Quantitative RNA mass/ volume values obtained for the control group and the field-exposed groups.

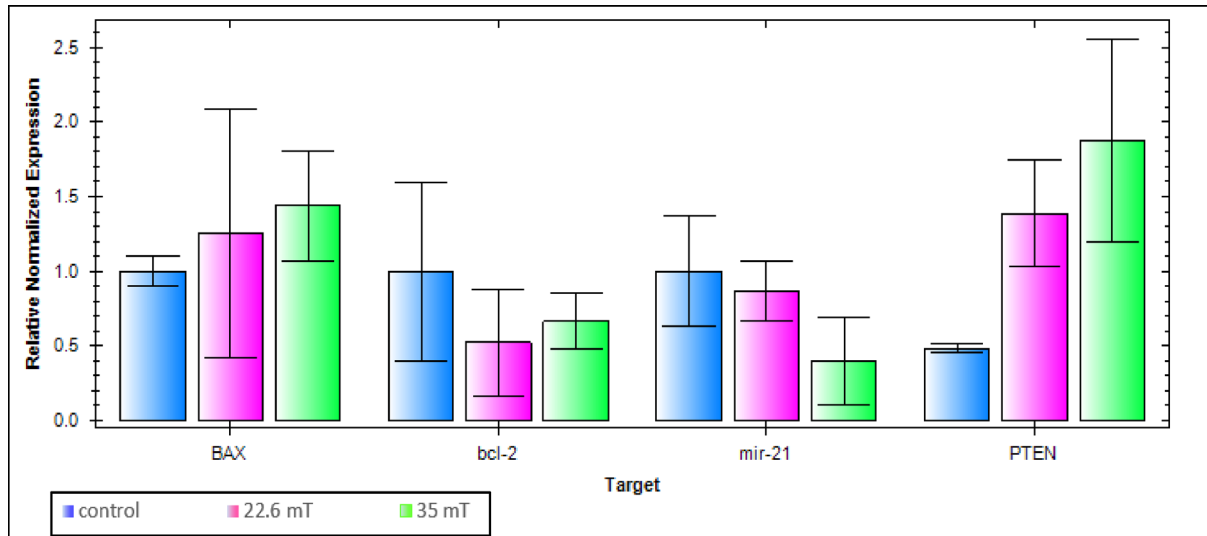


Fig. 12. The column chart of relative normalized expression values of BAX, BCL-2, and PTEN genes (relative to internal control gene GAPDH) as well as the results of MIR-21 gene expression values (relative to internal control gene SNORD) along with the error bars (their standard deviation (SD) values) for the control group and the groups under the field with intensities of 22.6 and 35 mT.

Oneway						
ANOVA						
		Sum of Squares	df	Mean Square	F	Sig.
BAX	Between Groups	.287	2	.143	.512	.623
BCL-2	Between Groups	.357	2	.179	1.031	.412
PTEN	Between Groups	2.971	2	1.486	7.470	.024
MIR-21	Between Groups	.593	2	.296	3.412	.102

Post Hoc Tests						
Multiple Comparisons						
LSD						
Dependent Variable	(I) Group	(J) Group	Mean Difference (I-J)	Std. Error	Sig.	95% Confidence Interval
BAX	1	2	-.250590000	.4319510027	.583	-.130753603 .8063560277
	1	3	-.435410000	.4319510027	.352	-.149235603 .6215360277
	2	1	.250590000	.4319510027	.583	-.806356028 1.307536028
	2	3	-.184820000	.4319510027	.684	-.124176603 .8721260277
	3	1	.435410000	.4319510027	.352	-.621536028 1.492356028
	3	2	.184820000	.4319510027	.684	-.872126028 1.241766028
BCL-2	1	2	.475090000	.3397389219	.211	-.356221194 1.306401194
	1	3	.333840000	.3397389219	.364	-.497471194 1.165151194
	2	1	-.475090000	.3397389219	.211	-.130640119 .3562211943
	2	3	-.141250000	.3397389219	.692	-.972561194 .6900611943
	3	1	-.333840000	.3397389219	.364	-.116515119 .4974711943
	3	2	.141250000	.3397389219	.692	-.690061194 .9725611943
PTEN	1	2	-.900730000*	.3641208417	.048	-.179170160 -.009758397
	1	3	-.138693000*	.3641208417	.009	-.227790160 -.495958397
	2	1	.900730000*	.3641208417	.048	.0097583971 1.791701603
	2	3	-.486200000	.3641208417	.230	-.137717160 .4047716029
	3	1	1.38693000*	.3641208417	.009	.4959583971 2.277901603
	3	2	.486200000	.3641208417	.230	-.404771603 1.377171603
MIR-21	1	2	.131690000	.2406467148	.604	-.457151298 .7205312983
	1	3	.598210000*	.2406467148	.047	.0093687017 1.187051298
	2	1	-.131690000	.2406467148	.604	-.720531298 .4571512983
	2	3	.466520000	.2406467148	.101	-.122321298 1.055361298
	3	1	-.598210000*	.2406467148	.047	-.18705130 -.009368702
	3	2	-.466520000	.2406467148	.101	-.105536130 1.223212983

Fig. 13. A screenshot of the results of the One-way ANOVA test in SPSS software on the significance of the difference in gene expression between the groups under ELF-EMF and the control group.

gene expression. However, if mutated, they become an "onco-miR" and are overexpressed. For example, miR-21, encoded by the MIR-21 gene, functions by inhibiting the expression of phosphatases (which limit the activity of signaling pathways). Since most of the targets of miR-21 are tumor suppressors, this microRNA has been associated with a variety of cancers, including breast, ovarian, cervical, colon, lung, prostate, brain, liver, esophagus, pancreas, and thyroid^{50,51}.

However, little information is available on the relevance of miR-21 for prostate cancer. A study by Stafford et al. in 2022 showed that high expression of miR-21 was significantly associated with prostate cancer. Therefore, miR-21 expression may be a useful prognostic biomarker in this disease⁵². Also, in a study by Folini et al. in 2010, the role of miR-21 and its potential as a therapeutic target were investigated in two prostate cancer cell lines, characterized by different levels of miR-21 expression and PTEN gene status. The results showed that miR-21 is not a major factor in the initiation of prostate cancer, and its damage is not a valuable therapeutic strategy in this disease. This supports the idea that the oncogenic properties of miR-21 may be cell and tissue-dependent and that the potential role of a given miRNA as a therapeutic target should be investigated according to the disease⁵³.

Figure 16 reveals the Real-time PCR output results showing the relative expression of the MIR-21 gene for the two groups under field intensities of 22.6 and 35 mT and the control group, as well as their standard deviation (SD) and one, two, or three stars for P-values. As could be seen in this figure, being a magnified version of Fig. 11 for the MIR-21 gene, applying fields with intensities of 22.6 and 35 mT at a constant frequency of 50 Hz for 30

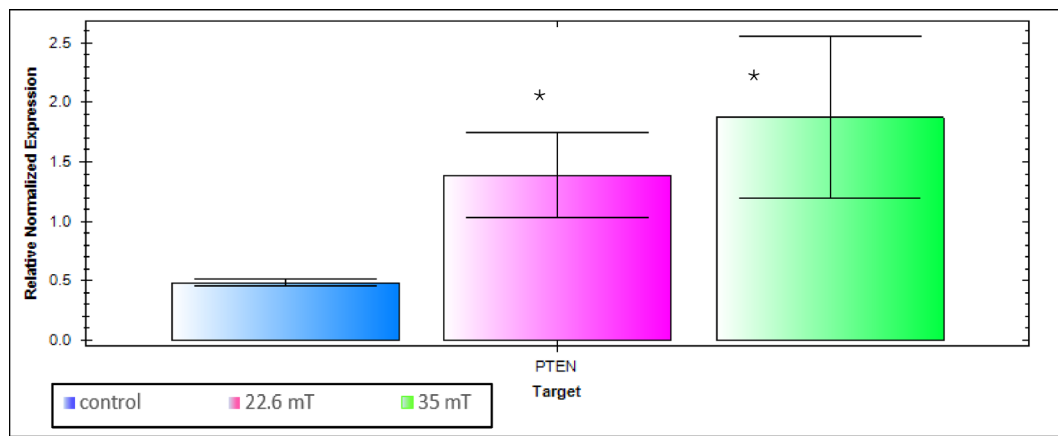


Fig. 14. Real-time PCR output results showing the relative expression of the PTEN gene for the two groups under field intensities of 22.6 and 35 mT and the control group, as well as their standard deviation (SD) and one, two, or three stars for *P*-values.

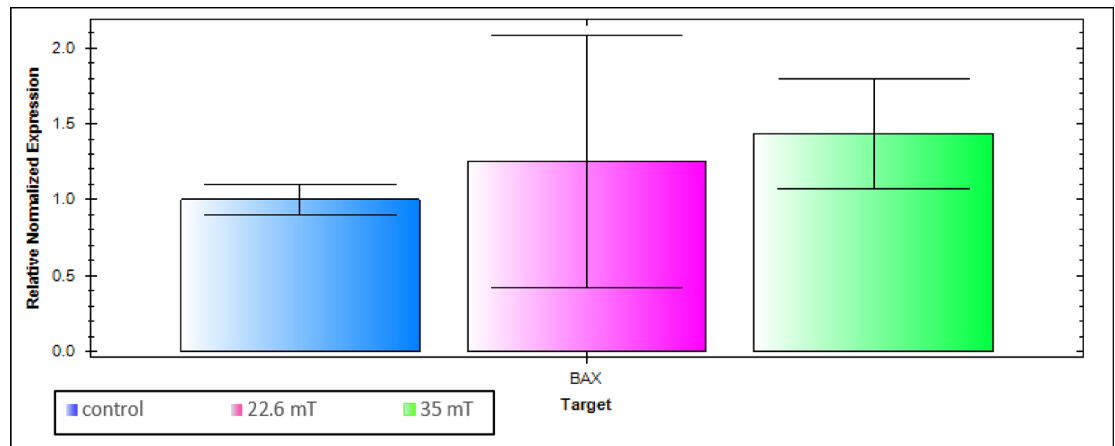


Fig. 15. Real-time PCR output results showing the relative expression of the BAX gene for the two groups under field intensities of 22.6 and 35 mT and the control group, as well as their standard deviation (SD).

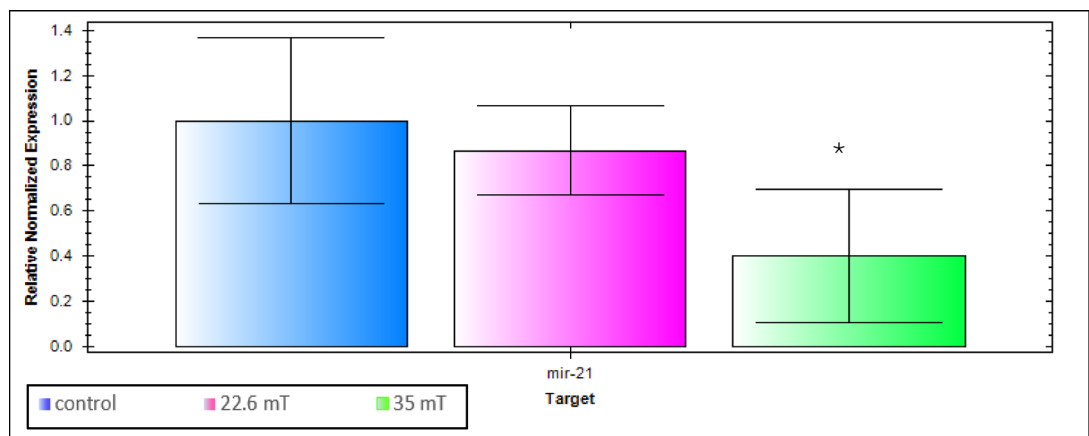


Fig. 16. Real-time PCR output results showing the relative expression of the MIR-21 gene for the two groups under field intensities of 22.6 and 35 mT and the control group, as well as their standard deviation (SD) and one, two, or three stars for *P*-values.

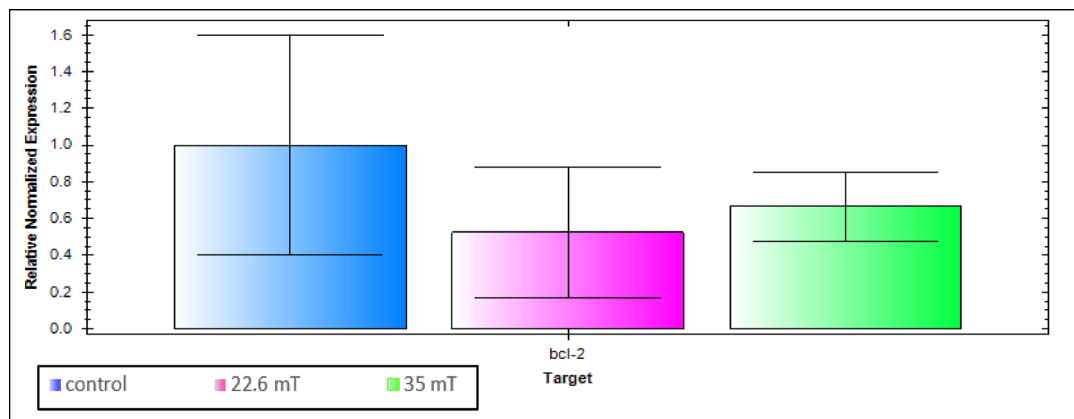


Fig. 17. Real-time PCR output results showing the relative expression of the BCL-2 gene for the two groups under field intensities of 22.6 and 35 mT and the control group, as well as their standard deviation (SD).

min resulted in a decrease in the expression of the MIR-21 gene (which acts as an onco-miR in prostate cancer), which is also significant at an intensity of 35 mT (*). Therefore, it can be said that applying fields with the above-mentioned intensities and frequencies is effective in reducing prostate cancer tumor growth, and the more the field intensity increases, the more the expression of this gene decreases.

It is worth noting that the BCL-2 gene is responsible for the production of regulatory proteins that regulate cell death (apoptosis) by inhibiting it (anti-apoptotic gene). It was the first apoptosis regulator to be identified in any living organism^{54,55}. Bcl-2 is located in the outer mitochondrial membrane, where it plays an important role in promoting cell survival and inhibiting the function of apoptosis-inducing proteins. Apoptosis-inducing proteins in the Bcl-2 family, including Bax and Bak, normally act on the mitochondrial membrane to increase permeability and release cytochrome c and ROS, which are important signals in the apoptotic cascade. These pro-apoptotic proteins are, in turn activated by Bh3 proteins and inhibited by Bcl-2 and Bcl-XI⁵⁶. Since cancer can be considered a disturbance in the homeostatic balance between cell growth and cell death, overexpression of anti-apoptotic genes and underexpression of genes involved in the induction of apoptosis can lead to the lack of programmed cell death that is characteristic of cancer. An example is seen in lymphomas. Overexpression of the anti-apoptotic protein Bcl-2 in lymphocytes alone does not cause cancer, but simultaneous overexpression of Bcl-2 and the proto-oncogene myc may cause aggressive B-cell malignancies, including lymphoma⁵⁷.

Figure 17 reveals the Real-time PCR output results showing the relative expression of the BCL-2 gene for the two groups under field intensities of 22.6 and 35 mT and the control group, as well as their standard deviation (SD). As can be understood from this figure, being a magnified version of Fig. 11 for the BCL-2 gene, applying a field with an intensity of 22.6 mT reduced the expression of this gene compared to the control group, but applying a field with a higher intensity of 35 mT increased the expression of this gene compared to the field with an intensity of 22.6 mT. Although the expression of this gene is still lower at the intensity of 35 mT compared to the control group, the difference in the relative expression of this gene is generally not significant. Considering that the BCL-2 gene blocks apoptosis, applying an electromagnetic field at a constant frequency of 50 Hz led to a decrease in the expression of this gene to some extent (if we consider the average amount of relative gene expression), which led to an increase in the rate of apoptosis in cancer cells and, as a result, a decrease in tumor growth to some extent, although in this regard, the field with a lower intensity of 22.6 mT was more effective than the field with a higher intensity of 35 mT.

Conclusion

By increasing the intensity of the ELF P-EMF from 22.6 to 35 mT and the duration of exposure from 30 to 60 min, the mortality rate of DU-145 cancer cells increases significantly, although, in terms of time, part of this increase in mortality is probably due to the increase in temperature. Also, the flow cytometry results indicate that exposure of DU-145 cells to ELF P-EMF with two intensities of 22.6 and 35 mT for 30 min can induce apoptosis in these cells.

In addition, applying the field with the mentioned conditions significantly increased the expression of the PTEN tumor suppressor gene, and therefore, it can be said that applying the field with the mentioned intensities and frequencies is effective in suppressing prostate cancer tumors.

Furthermore, applying the field with the mentioned conditions is effective in inducing apoptosis of prostate cancer cells by the BAX gene and reducing tumor growth to some extent.

Besides, considering that applying the field with these conditions leads to a significant decrease in the expression of the MIR-21 gene, which acts as an oncomir in prostate cancer, it can be said that applying the field with the aforementioned intensities and frequencies is effective in reducing prostate cancer tumor growth.

Moreover, since the BCL-2 gene blocks apoptosis, applying electromagnetic fields under the aforementioned conditions has led to a decrease in the expression of this gene to some extent, which in turn leads to an increase in the rate of apoptosis in cancer cells and a decrease in tumor growth to some extent.

To find the optimal frequency, the cells should be repeatedly exposed to fields with different frequencies, and then the MTT test should be performed. The field intensity, duration of exposure, and the position of the coil in relation to the cells should also be changed to determine the optimal conditions and frequency. Therefore, the number of experiments, their cost, and the time to perform them will rise significantly, which should be considered in future research.

A complete study of the effect of electromagnetic fields on the human body will be possible when the field with the intensity, time, and frequencies mentioned in this study is also examined on healthy and normal prostate gland cells. Because if body tissue is exposed to an electromagnetic field as a treatment, healthy tissue will also be exposed to it, and therefore, the treatment should have minimal negative effects on healthy tissue and only target cancer cells.

For a more complete study, the effects of low-frequency electromagnetic fields on the expression of other key genes, such as P53, MIR-29, and other microRNAs, B2M, etc., in prostate cancer and other cancers with different intensities, frequencies, and exposure times can be studied.

Data availability

The data that support the findings of this study are available from the corresponding author upon reasonable request.

Received: 20 February 2025; Accepted: 17 September 2025

Published online: 27 October 2025

References

1. National Cancer Institute (NCI). *SEER Cancer Stat Facts: Prostate Cancer* <https://seer.cancer.gov/statfacts/html/prost.html> (2023).
2. World Cancer Research Fund (WCRF). *Prostate cancer statistics* <https://www.wcrf.org/preventing-cancer/cancer-statistics/prostate-cancer-statistics/> (2024).
3. Koziorowska, A., Romerowicz-Misielak, M., Sołek, P. & Koziorowski, M. Extremely low-frequency variable electromagnetic fields affect cancer and noncancerous cells in vitro differently: Preliminary study. *Electromagn. Biol. Med.* **37**(1), 35–42. <https://doi.org/10.1080/15368378.2017.1414057> (2018).
4. Filipovic, N. et al. Electromagnetic field investigation on different cancer cell lines. *Cancer Cell Int.* **14**, 84. <https://doi.org/10.1186/s12935-014-0084-x> (2014).
5. Grassi, C. et al. Effects of 50Hz electromagnetic fields on voltage-gated Ca²⁺ channels and their role in modulation of neuroendocrine cell proliferation and death. *Cell Calcium* **35**, 307–315. <https://doi.org/10.1016/j.ceca.2003.10.001> (2004).
6. Simkó, M. et al. Effects of 50 Hz EMF exposure on micronucleus formation and apoptosis in transformed and nontransformed human cell lines. *Bioelectromagnetics* **19**, 85–91 (1998).
7. Simkó, M. Induction of cell activation processes by low-frequency electromagnetic fields. *Sci. World J.* **4**, 4–22. <https://doi.org/10.1100/tsw.2004.175> (2004).
8. Sadooghi, S. D. Investigating the effects of low-frequency electromagnetic field on HT-29 cancer cell line. *Feyz.* **17**(5), 413–421 (2013).
9. Sadooghi, S. D. et al. Investigating the effects of low-frequency electromagnetic field on MCF-7 cancer cell line. *Stud. Med. Sci.* **25**(5), 444–452 (2014).
10. Pasi, F. et al. Pulsed electromagnetic field with temozolomide can elicit an epigenetic pro-apoptotic effect on glioblastoma T98G cells. *Anticancer Res.* **36**, 5821–5826 (2016).
11. Ren, J. et al. LF-MF inhibits iron metabolism and suppresses lung cancer through activation of P53-miR-34a-E2F1/E2F3 pathway. *Sci. Rep.* **7**, 749. <https://doi.org/10.1038/s41598-017-00853-x> (2017).
12. Xu, Y. et al. Low-frequency magnetic fields induce autophagy-associated cell death in lung cancer through miR-486-mediated inhibition of Akt/mTOR signaling pathway. *Sci. Rep.* **7**, 11776. <https://doi.org/10.1038/s41598-017-12109-9> (2017).
13. Calabro, E. & Magazù, S. New perspectives in the treatment of tumor cells by electromagnetic radiation at resonance frequencies in cellular membrane channels. *Open Biotechnol. J.* **13**(1), 105–110. <https://doi.org/10.2174/187407070190130105> (2019).
14. Barati, M. et al. 1Hz 100mT electromagnetic field induces apoptosis in breast cancer cells through up-regulation of P38 and P21. *Multidiscip. Cancer Investig.* **4**(1), 23–29 (2020).
15. Shayeghan, M. et al. Effect of extremely low-frequency electromagnetic field on apoptosis induction and expression of estrogen receptor, progesterone receptor, and ERBB2 in BT-474 cells. *Iran J. Breast Dis.* **15**(2), 36–49 (2022).
16. Pantelis, P. et al. Pulsed electromagnetic fields (PEMFs) trigger cell death and senescence in cancer cells. *Int. J. Mol. Sci.* **25**(5), 2473. <https://doi.org/10.3390/ijms25052473> (2023).
17. Barbault, A. et al. Amplitude-modulated electromagnetic fields for the treatment of cancer: Discovery of tumor-specific frequencies and assessment of a novel therapeutic approach. *J. Exp. Clin. Cancer Res.* **28**, 51. <https://doi.org/10.1186/1756-9966-28-51> (2009).
18. Halliday, D., Resnick, R. & Walker, J. *Fundamentals of Physics* 8th edn. (Wiley, 2005).
19. Meeker, D. *Finite Element Method Magnetics Version 4.2 User's Manual* (2018).
20. Stockert, J. C. et al. MTT assay for cell viability: Intracellular localization of the formazan product is in lipid droplets. *Acta Histochem.* **114**(8), 785–796. <https://doi.org/10.1016/j.acthisi.2012.01.006> (2012).
21. Stockert, J. C. et al. Tetrazolium salts and formazan products in cell biology: Viability assessment, fluorescence imaging, and labeling perspectives. *Acta Histochem.* **120**(3), 159–167. <https://doi.org/10.1016/j.acthisi.2018.02.005> (2018).
22. Cory, A. H. et al. Use of an aqueous soluble tetrazolium/formazan assay for cell growth assays in culture. *Cancer Commun.* **3**(7), 207–212. <https://doi.org/10.3727/095535491820873191> (1991).
23. Bio-Rad Laboratories. *Lysis Buffer* <https://www.bio-rad.com> (2024).
24. Pars Tous. *Total RNA Extraction Kit*. <https://parstous.com/product/total-rna-extraction-kit-2/>.
25. Oswald, N. *Ethanol precipitation of DNA and RNA: How it works* (Bitesize Bio, 2024).
26. Haddad, F. & Baldwin, K. M. Reverse transcription of the ribonucleic acid: The first step in RT-PCR assay. *Methods Mol. Biol.* **630**, 261–270. https://doi.org/10.1007/978-1-60761-629-0_17 (2010).
27. BioSistemika. qPCR, Microarrays or RNA Sequencing - What to Choose? <https://www.biosistemika.com/blog/qpcr-microarrays-rna-sequencing-choose-one/> (2017).
28. Pars Tous. *Supra cDNA Synthesis Kit*. <https://parstous.com/product/>.
29. Zhong, Q. et al. Expression profiling and validation of potential reference genes during *Paralichthys olivaceus* embryogenesis. *Mar. Biotechnol.* **10**, 310–318. <https://doi.org/10.1007/s10126-007-9068-3> (2008).
30. Bustin, S. A. Absolute quantification of mRNA using real-time reverse transcription polymerase chain reaction assays. *J. Mol. Endocrinol.* **25**, 169–193 (2000).

31. Joshi, C. J. et al. What are housekeeping genes?. *PLoS Comput. Biol.* **18**(7), e1010295. <https://doi.org/10.1371/journal.pcbi.1010295> (2022).
32. Sikand, K. et al. Housekeeping gene selection advisory: Glyceraldehyde-3-phosphate dehydrogenase (GAPDH) and β -actin are targets of miR-644a. *PLoS ONE* **7**(10), e47510. <https://doi.org/10.1371/journal.pone.0047510> (2012).
33. Avgeris, M. et al. The loss of the tumor-suppressor miR-145 results in the shorter disease-free survival of prostate cancer patients. *Br. J. Cancer* **108**(12), 2573–2581. <https://doi.org/10.1038/bjc.2013.250> (2013).
34. Saini, S. et al. Regulatory role of miR-203 in prostate cancer progression and metastasis. *Clin. Cancer Res.* **17**(16), 5287–5298. <https://doi.org/10.1158/1078-0432.CCR-10-2619> (2011).
35. Suh, S. O. et al. MicroRNA-145 is regulated by DNA methylation and p53 gene mutation in prostate cancer. *Carcinogenesis* **32**(5), 772–778. <https://doi.org/10.1093/carcin/bgr036> (2011).
36. SinaClon Bioscience. <https://sinaclon.com>.
37. Ali, M. R. et al. Targeting heat shock protein 70 using gold nanorods enhances cancer cell apoptosis in low dose plasmonic photothermal therapy. *Biomaterials* **102**, 1–8. <https://doi.org/10.1016/j.biomaterials.2016.06.017> (2016).
38. Song, A. S. et al. Thermally induced apoptosis, necrosis, and heat shock protein expression in three-dimensional culture. *J. Biomed. Eng.* **136**, 071006. <https://doi.org/10.1115/1.4027272> (2014).
39. Zhu, X. et al. Temperature-feedback upconversion nanocomposite for accurate photothermal therapy at facile temperature. *Nat. Commun.* **7**, 10437. <https://doi.org/10.1038/ncomms10437> (2016).
40. Steck, P. A. et al. Identification of a candidate tumor suppressor gene, MMAC1, at chromosome 10q23.3 that is mutated in multiple advanced cancers. *Nat. Genet.* **15**(4), 356–362. <https://doi.org/10.1038/ng0497-356> (1997).
41. Luongo, F. et al. PTEN tumor-suppressor: The dam of stemness in cancer. *Cancers* **11**(8), 1076. <https://doi.org/10.3390/cancers11081076> (2019).
42. Thompson, C. B. Apoptosis in the pathogenesis and treatment of disease. *Science* **267**, 1456–1462. <https://doi.org/10.1126/science.7878464> (1995).
43. Melino, G. The Sirens' song. *Nature* **412**, 23. <https://doi.org/10.1038/35083653> (2001).
44. NCBI. *Entrez Gene: BCL2-associated X protein, Gene ID: 581* <https://www.ncbi.nlm.nih.gov/gene/581> (2024).
45. Gao, C. & Wang, A. Y. Significance of increased apoptosis and Bax expression in human small intestinal adenocarcinoma. *J. Histochem. Cytochem.* **57**(12), 1139–1148. <https://doi.org/10.1369/jhc.2009.954446> (2009).
46. Hemann, M. & Lowe, S. W. The p53-Bcl-2 connection. *Cell Death Differ.* **13**, 1256–1259. <https://doi.org/10.1038/sj.cdd.4401962> (2006).
47. Janic, A. et al. Decoding p53 tumor suppression: A crosstalk between genomic stability and epigenetic control?. *Cell Death Differ.* <https://doi.org/10.1038/s41418-024-01259-9> (2024).
48. Wallace-Brodeur, R. R. & Lowe, S. W. Clinical implications of p53 mutations. *Cell Mol. Life Sci.* **55**, 64–75. <https://doi.org/10.1007/s00180050270> (1999).
49. Sjöström, J. & Bergh, J. How apoptosis is regulated, and what goes wrong in cancer. *BMJ* **322**(7301), 1538–1539. <https://doi.org/10.1136/bmj.322.7301.1538> (2001).
50. Volinia, S. et al. A microRNA expression signature of human solid tumors defines cancer gene targets. *Proc. Natl. Acad. Sci. USA* **103**(7), 2257–2261. <https://doi.org/10.1073/pnas.0510565103> (2006).
51. Kumaraswamy, R. et al. Regulation and function of miRNA-21 in health and disease. *RNA Biol.* **8**(5), 706–713. <https://doi.org/10.4161/rna.8.5.16154> (2011).
52. Stafford, M. Y. C. et al. Prognostic value of miR-21 for prostate cancer: A systematic review and meta-analysis. *Biosci. Rep.* **42**(1), BSR20211972 (2022).
53. Folini, M. et al. miR-21: An oncomir on strike in prostate cancer. *Mol. Cancer* **9**, 12. <https://doi.org/10.1186/1476-4598-9-12> (2010).
54. Tsujimoto, Y. et al. Cloning of the chromosome breakpoint of neoplastic B cells with the t(14;18) chromosome translocation. *Science* **226**(4678), 1097–1099. <https://doi.org/10.1126/science.6093263> (1984).
55. Cleary, M. L. et al. Cloning and structural analysis of cDNAs for bcl-2 and a hybrid bcl-2/immunoglobulin transcript resulting from the t(14;18) translocation. *Cell* **47**(1), 19–28. [https://doi.org/10.1016/0092-8674\(86\)90362-4](https://doi.org/10.1016/0092-8674(86)90362-4) (1986).
56. Hardwick, J. M. & Soane, L. Multiple functions of BCL-2 family proteins. *Cold Spring Harb. Perspect. Biol.* **5**(2), a008722. <https://doi.org/10.1101/cshperspect.a008722> (2013).
57. Otake, Y. et al. Overexpression of nucleolin in chronic lymphocytic leukemia cells induces stabilization of bcl2 mRNA. *Blood* **109**(7), 3069–3075. <https://doi.org/10.1182/blood-2006-08-043257> (2007).

Author contributions

Abouzar Bahari: wrote the main manuscript text, figures, and tables, and reviewed it. Javad Baharara and Khadijeh Nejad Shahrokhabadi: checked, verified, and reviewed the manuscript results and text Maryam Lotfi: made lab tests and prepared figures.

Funding

There is no funding for this research.

Declarations

Competing interests

The authors declare no competing interests.

Additional information

Correspondence and requests for materials should be addressed to A.B.

Reprints and permissions information is available at www.nature.com/reprints.

Publisher's note Springer Nature remains neutral with regard to jurisdictional claims in published maps and institutional affiliations.

Open Access This article is licensed under a Creative Commons Attribution-NonCommercial-NoDerivatives 4.0 International License, which permits any non-commercial use, sharing, distribution and reproduction in any medium or format, as long as you give appropriate credit to the original author(s) and the source, provide a link to the Creative Commons licence, and indicate if you modified the licensed material. You do not have permission under this licence to share adapted material derived from this article or parts of it. The images or other third party material in this article are included in the article's Creative Commons licence, unless indicated otherwise in a credit line to the material. If material is not included in the article's Creative Commons licence and your intended use is not permitted by statutory regulation or exceeds the permitted use, you will need to obtain permission directly from the copyright holder. To view a copy of this licence, visit <http://creativecommons.org/licenses/by-nc-nd/4.0/>.

© The Author(s) 2025